

Vibration signals at the early stage of fouling in reverse osmosis system

Minseok Kim, Noori Kim, Jongmin Jeon, Suhan Kim*

Department of Civil Engineering, Pukyong National University, 45 Yongso-ro, Nam-gu, Busan 48513, Korea,
Tel. +82-51-629-6065; Fax: +82-51-629-6063; email: suhankim@pknu.ac.kr (S. Kim)

Received 23 August 2019; Accepted 26 November 2019

ABSTRACT

For the first time, the approach to detect early fouling in reverse osmosis (RO) system by vibration sensor is introduced. The vibration sensor attached to the high-pressure pump collects the vibration data of the RO system, which are affected by foulants accumulated on the membrane surface. Lab-scale fouling tests were carried out using humic acid in two different approaches: the constant-control test and the variation test, where the former is to maintain the constant test conditions and the latter is to intentionally change some test conditions during the fouling test. The vibration sensor collected three-axis vibration data 8,192 data points per second and the size of the data file is about one gigabyte per hour. The raw data files were trimmed to smaller-sized files (six vibration data-sets per one fouling test) using R version 3.5.1 for the fouling analysis. The vibration data analyses for both the constant-control and variation tests revealed that some of six vibration data-sets could be used to figure out the early fouling even in the test condition in variation, where the early fouling is defined as the period when the average of the vibration data drops by over some percentage compared to that in no-fouling period.

Keywords: Reverse osmosis (RO); Fouling; Vibration sensor

1. Introduction

Fouling is a key factor to design and operate reverse osmosis (RO) system [1–4]. It is very important to detect the early stage of fouling, otherwise, it could be difficult to remove foulants on the membrane surface to recover the performance of RO membranes [5]. In general, fouling can be detected by a decrease in water flux (for constant pressure operation mode) or an increase in applied pressure (for constant flux operation mode).

However, these hydrodynamic parameters (i.e., water flux and applied pressure) are affected by not only fouling but also other factors (e.g., feed water temperature and salt concentration) [6,7]. For example, water flux (for constant pressure operation mode) decreases as feed temperature decreases because the viscosity of feed water increases and water permeability of membrane decreases. If salt

concentration increases, the water flux decreases because of the osmotic pressure of feed-concentrate increases. Thus, water flux (for constant pressure operation mode) or applied pressure (for constant pressure operation mode) are always fluctuated during the operation even if fouling does not occur, which is the reason why it is difficult to detect the early stage of fouling in real field applications of RO system.

A normalized parameter such as normalized permeate flow rate suggested by ASTM D 4516 could be a solution [8]. Normalized permeate flow rate and permeate salt concentration from ASTM D 4516 reflect changes by feedwater temperature and salt concentration, which means ‘theoretically’ the normalized parameters are not changed by changes in feed water temperature and salt concentration. Thus, a decrease in the normalized parameters means fouling occurs in the system. However, it is reported that the normalization

* Corresponding author.

method did not work very well in a real situation due to the fluctuation of the normalized parameters [9,10].

Although there are lots of research papers about detecting the early fouling in RO systems [11–14], detecting the early fouling in the environment where feed water temperature and salt concentration have fluctuated like real field applications is not seriously considered. One research paper published by our research group [6] introduces a corrected normalized permeate flux to enhance the applicability of the ASTM normalization method by decreasing the fluctuation of the normalized parameters. However, the corrected normalized permeate flux needs a fitting process that requires operation data obtained in a no-fouling condition.

In this work, a new early fouling detection method by analyzing vibration signals of the RO system is proposed. If fouling occurs, the feed channel shape will change because of the foulants accumulated on the membrane surface (Fig. 1). This induces a higher resistance to the feed flow and may cause changes in vibrating patterns of the membrane module. If a vibration sensor is installed in the RO system, the changed vibrating patterns of the membrane module when fouling occurs could be observed. This is the hypothesis of this research work.

Since high-pressure pumps are one of the most expensive parts in real-scale RO systems, vibration sensors are often installed in the pumps to predict any defects of the pumps such as flow blockages and cavitation [15–17]. The vibration signals collected by the vibration sensor become abnormal if there happen some problems in the pump. The abnormal signals can make operators stop the system and inspect the pump. Our idea is the collected vibration data may give a fouling alarm if the shrunk feed channel by accumulated foulants on the membrane surface (Fig. 1) induces enough friction to produce a distinguished vibration signal.

The concept of vibration to reduce membrane fouling has often been applied to the researches related to membrane technology [18], but any research results using

vibration sensors to detect the early fouling are hardly observed. To our best knowledge, this paper will be the first one to introduce vibration sensors to alarm the early fouling in an RO system.

2. Methods

2.1. Lab-scale fouling test

A lab-scale fouling test was carried out using an RO system described in Fig. 2 and the procedure described elsewhere [19]. The vibration sensor used in this work was a triaxial sensor called FASTTRACER (Sequoia IT S.R.L., Italy) [20], and it was attached to the upper side of the high-pressure pump as shown in Fig. 2. Sodium chloride (99.999% refined NaCl, OCI Co. Ltd., China) was used to control salt concentration in feed water and humic acid (Wako Pure Chemical Industries, Ltd., Japan) was used as a model foulant. The membrane coupon used in this work was taken from RE4040-FEN, Toray Chemical Korea.

At the start of each fouling test, feed water was prepared using pure water obtained from tap water filtered by a 4-inch RO module system (RE4040-SHN, Toray

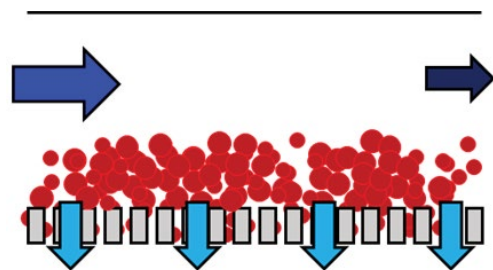


Fig. 1. Feed-concentrate channels in the RO membrane become narrowed in the presence of fouling.

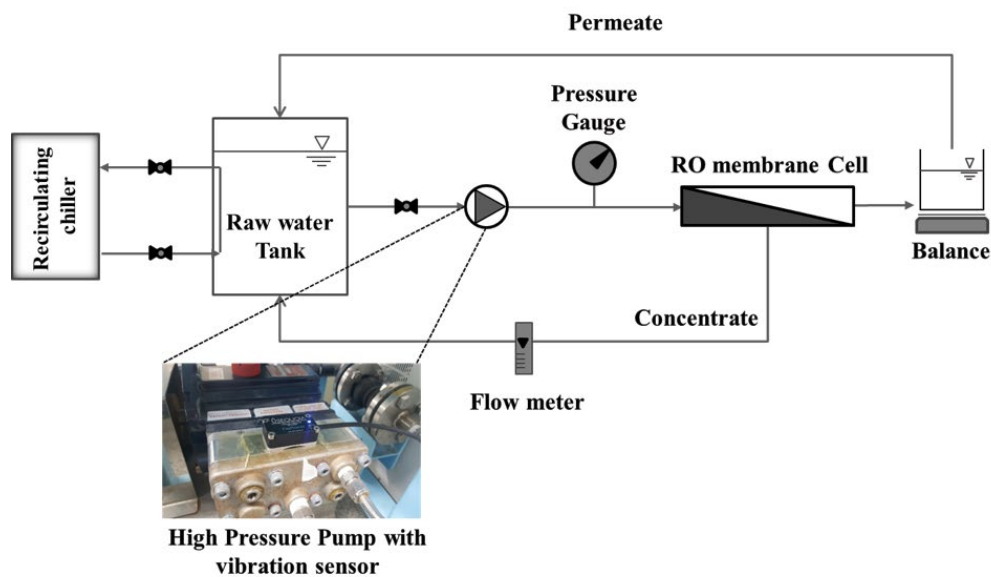


Fig. 2. Lab-scale RO system with vibration sensor [19].

Chemical Korea) and the initial salt concentration was set to 2,000 mg/L using sodium chloride. 100 mg/L of humic acid was spiked to the raw water tank after a stabilization period of about 1 d to obtain stable vibration signals and to maintain constant permeate flux (~22 LMH at 7.6–8.0 bar) and temperature (~20°C).

Two different types of fouling tests were carried out; one is called the constant-control test and the other is called the variation test. The objective of the constant-control test is to limit the factors affecting the permeate flux to the addition of humic acid. If flux decline starts from a certain period in the constant-control test, this period is considered as the early stage of fouling. In the constant-control test, all the operating conditions including raw water temperature, salt concentration, and applied pressure was maintained at the initial values to prevent these parameters from affecting any changes in flux.

However, as mentioned in introduction, the operation parameters (e.g., temperature and salt concentration) are fluctuated during the operation in real field applications, and one cannot easily find out the starting point of fouling by flux decline only because various factors such as the decrease in temperature, the increase in salt concentration, and the fouling can affect the flux decline. The objective of this work is to investigate the potential of analyzing vibration data to identify the early stage of fouling in a real field situation where all the operation parameters fluctuate. Thus, in the variation test, salt concentration keeps changed by randomly adding sodium chloride (to increase) or pure water (to decrease) during the operation. In this condition, it is difficult to find the starting point of fouling by observing the change in permeate flux. The purpose of the variation test is to investigate if the vibration signals can detect the starting point of fouling despite changes in operating conditions such as the salt concentration of raw water.

2.2. Pretreatment of the vibration data

FASTTRACER, the vibration sensor used in this work can collect three-axis vibration data up to 8192 data points per second and the size of the vibration data is big enough to be about one gigabyte per hour. Thus, a data-downsizing procedure (called 'pretreatment' in this paper) should necessary to analyze the vibration signal to find out the starting point of fouling (i.e., the time when humic acid is spiked). When a fouling test is finished, raw data can be extracted using FT analyzer software (Sequoia IT S.R.L., Italy) [20] provided by the manufacturer of the vibration sensor. Since the test period is longer than 30 h, the vibration data file size is larger than 30 gigabytes, which cannot be opened using a spreadsheet program like Microsoft Excel. Therefore, we have used R version 3.5.1 [21] to open the big vibration data file and to decrease the file size for the analysis. In this work, one representative value of 8,192 data for the 1 s period was extracted using two different approaches; (1) maximum amplitude (MA) and (2) standard deviation (STD), which were selected to indirectly express the size of amplitude of vibration patterns like periodic functions as shown in Fig. 3. MA was calculated by subtracting the minimum value from the maximum value taken from the same 1 s period.

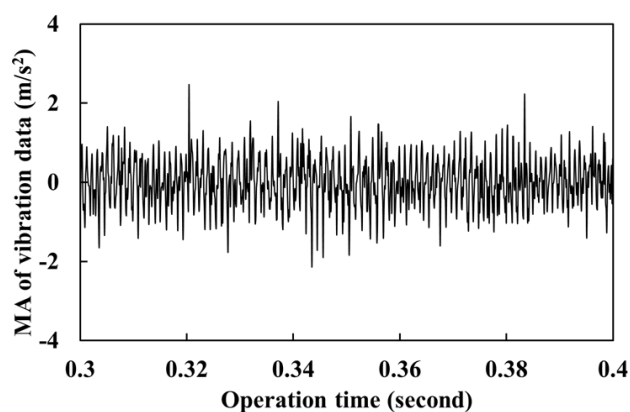


Fig. 3. An example of vibration data collected for a 0.1 s period.

3. Results and discussion

3.1. Vibration data analysis during the constant-control test

The objective of the constant-control test with a vibration sensor is to check if the vibration signal is changed due to fouling. Fig. 4 shows changes in permeate flux and salt rejection during the test. The total test period is divided into two: (1) the stabilization period with no fouling (no-fouling period) and (2) the fouling period. As indicated using an arrow, humic acid of 100 mg/L was added after 1,295 min from the beginning of the test, which means the fouling period starts at 1,295 min. Interestingly, a significant amount of flux decline was not observed after spiking humic acid (Fig. 4a). This can be explained by the concept of cake enhanced concentration polarization (CECP), which means the fouling (cake) layer enhances concentration polarization and it is the main reason for flux decline in the RO membrane filtration [3]. The effect of CECP gets higher as salt concentration and initial flux become higher. The constant-control test condition includes a salt concentration of 2,000 mg/L as NaCl and initial flux of 22 LMH, which are smaller than the experimental condition (e.g., seawater and initial flux of 28 LMH) in the literature about CECP [3]. Thus, the effect of CECP was not high enough to induce a noticeable flux decline as seen in Fig. 4a. The salt rejection was consistently decreased after humic acid is spiked as shown in Fig. 4b because the humic acid fouling layer enhances concentration polarization which results in the increase of salt concentration on the membrane surface. Although the initial salt rejection (~98%) is less than the nominal salt rejection (>99%) of the RE4040-FEN membrane, it is often observed in membrane coupons taken from membrane roll provided by membrane manufacturer and it does not mean any defect of the membrane [3].

Vibration data were collected during the constant-control test. After the experiment, a data file of 37.2 gigabytes was generated using FT analyzer software and it was trimmed to a file of 67.3 megabytes where all the data but MA and STD per each 1 s period were deleted. Since the vibration sensor collects three-axis data, six vibration data-sets (MA and STD of each axis) can be obtained for the fouling analysis as shown in Fig. 5. All the vibration data except the STD of the x -axis (Fig. 5d) shows significant fluctuating patterns.

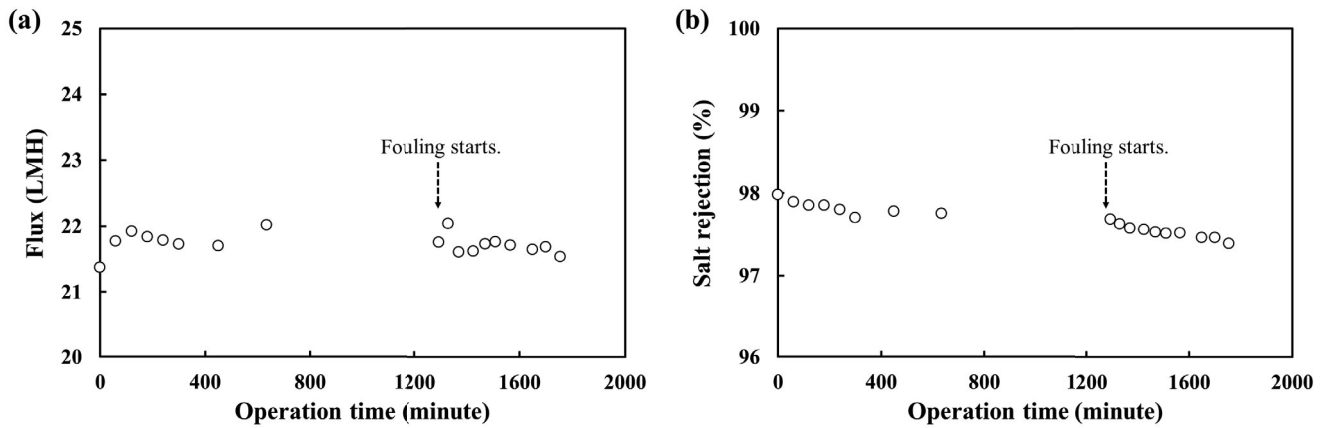


Fig. 4. (a) Permeate flux and (b) salt rejection during the constant-control test (humic acid 100 mg/L, NaCl 2,000 mg/L, initial permeate flux = 22 LMH at 7.6 bar).

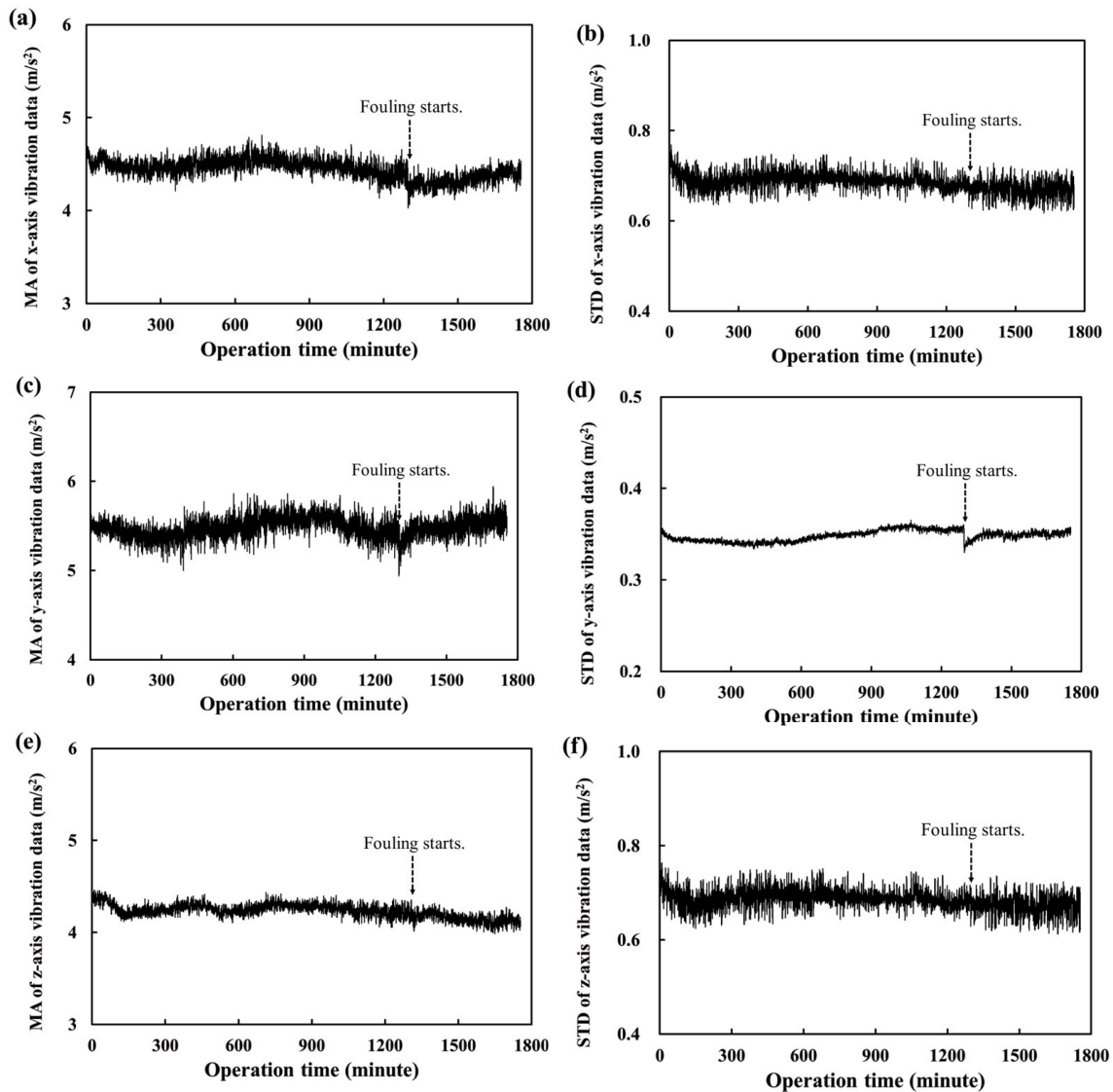


Fig. 5. Vibration data during the constant-control test (a) MA of x-axis vibration data, (b) STD of x-axis vibration data, (c) MA of y-axis vibration data, (d) STD of y-axis vibration data, (e) MA of z-axis vibration data, and (f) STD of z-axis vibration data.

It is difficult to figure out the starting point of fouling when the degree of the fluctuation is higher than the change of the vibration data due to fouling as shown in Figs. 5b, e, and f.

In Figs. 5a and c, a little noticeable drop of the vibration data were observed after humic acid was spiked. However, it may be difficult to figure out the starting point of fouling without knowing the answer first. For example, vibration data around 1,080 min of operation time shows a similar pattern to those around 1,300 min just after fouling started (Fig. 5c). In this case, chances are 1,080 min may be regarded as the starting point of fouling instead of 1,300 min.

In the case of an MA of x -axis vibration data (Fig. 5a), a similar pattern of vibration data to the fouling signal (i.e., a sudden drop around 1,300 min of operation time) is not observed in the no-fouling period (<1,295 min). To apply the vibration data to detect early fouling, it is important to define the fouling signal pattern to distinguish it from the vibration patterns of the no-fouling period. For example, the starting point of fouling can be defined as the time when the vibration signals like MA and STD drop by over some percentage (e.g., >5%) of the average of the vibration data in the no-fouling period. The average MA of x -axis vibration data in the no-fouling period is 4.49 m/s² while that in the period when the fouling signal appears (1,298–1,302 min) is 4.09 m/s² (i.e., 8.8% drop).

The fouling signal appears in the STD of y -axis vibration data (Fig. 5d). The average STD of y -axis vibration data in the no-fouling period is 0.36 m/s² while that in the period when the fouling signal appears (1,298–1,302 min) is 0.33 m/s² (i.e., 8.3% drop). The fouling signal seems clearer in Fig. 5d than that in Fig. 5a, although the difference in percentage between the average values of vibration data in the no-fouling period and that in the period when the fouling signal appears is similar. This is because of the degree of fluctuation in Fig. 5d is much smaller than that in Fig. 5a.

The vibration data analysis so far reveals: (1) the period when fouling signal appears can be defined as the period when the average of the vibration data drops by over some percentage compared to that in the no-fouling period. (2) Two of the six vibration data-sets (Figs. 5a and d) can be used to figure out the fouling signal while the fouling signal is hardly observed in the other data-sets (Figs. 5b, c, e, and f).

Therefore, we may set a rule to determine an early fouling period from the vibration data such as: If the fouling signal (defined in (1)) is observed in at least one of the six vibration data-sets, the period when the fouling signal occurs can be identified as the early stage of fouling. However, more fouling tests with vibration data should be carried out to confirm the rule to determine an early fouling period.

3.2. Vibration data analysis during the variation test

In section 3.1, it was proved that vibration data can be used to detect early fouling in the constant-control test. The next step is to find out if vibration data can detect early fouling in the operation condition where some parameters such as temperature and salt concentration in the feed are fluctuated like real field applications. Fig. 6 shows changes in permeate flux and salt rejection during the test. Total test period is divided into three: (1) the stabilization period with no fouling in a constant-control condition (NaCl 2,000 mg/L), (2) no-fouling period with varying salt concentration (NaCl 1,223–3,315 mg/L), and (3) the fouling period after humic acid of 100 mg/L is spiked (after 1,710 min of operation time).

Flux decreases as salt concentration decrease because of the decreased osmotic pressure in the feed. Since salt concentration is randomly changed in the no-fouling period with varying salt concentration, flux went randomly up and down in constant operating pressure of 8.0 bar as shown in Fig. 6a. Without the arrow indicating the starting point of fouling, one cannot figure out when fouling starts due to the flux fluctuation. Salt rejection decreases at a higher salt concentration in the feed because of the salt diffusion rate through membrane increases as salt concentration in the vicinity of membrane surface increases. This is the reason why salt rejection also fluctuated like the case of flux, but it was gradually decreased while fluctuating after the starting point of fouling (Fig. 6b). Hence, the occurrence of fouling may be expected by observing a significant drop of salt rejection although the starting point is not figured out.

Vibration data were also collected during the variation test. After the experiment, a data file of 34.0 gigabytes was generated using FT analyzer software and it was trimmed to

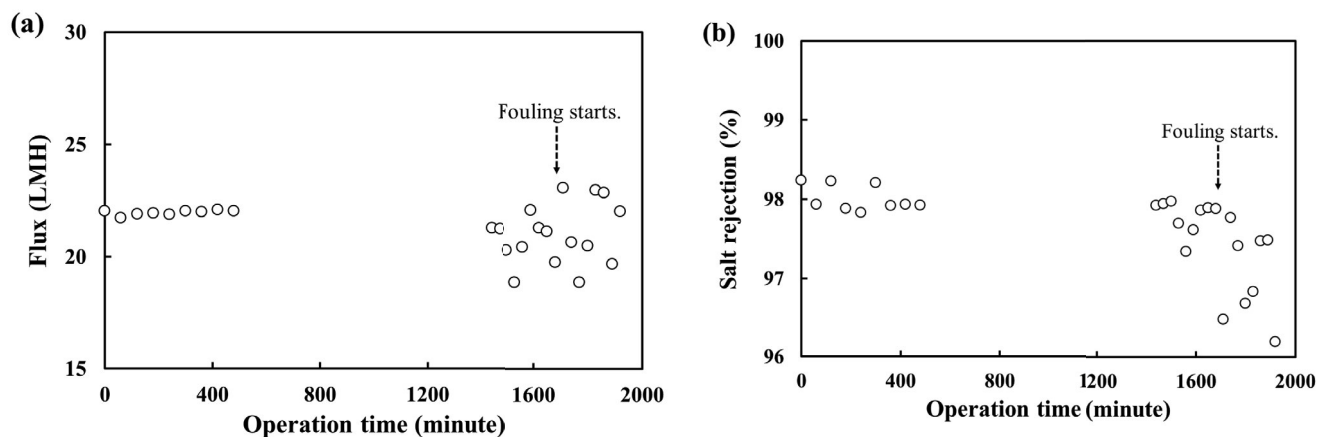


Fig. 6. (a) Permeate flux and (b) salt rejection during the variation test (humic acid 100 mg/L, NaCl 1,223–3,315 mg/L, initial permeate flux = 22 LMH at 8.0 bar).

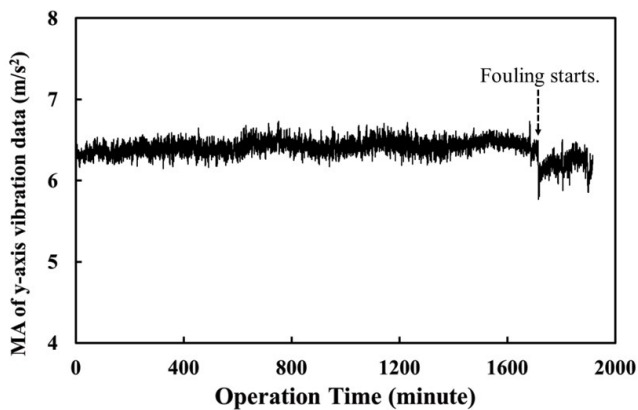


Fig. 7. Vibration data during the variation test MA of *y*-axis vibration data.

a file of 69.4 megabytes where all the data but MA and STD per each 1 s period were deleted. Among the six vibration data-sets, the MA of *y*-axis vibration data is shown in Fig. 7, where the fouling signal appears clearly. The average of the vibration data in the period the fouling signal appears (1,715–1,718 min) was 5.92 m/s² and that in the no-fouling period was 6.42 m/s², which means 7.8% drop of the vibration data in a short period after fouling started. Moreover, the period when the salt concentration in feed was fluctuated without fouling (1,438–1,710 min) did not show any distinguishable change in the vibration data, which means the vibration signal does not respond to changes of salt concentration in the feed, but the occurrence of fouling. This is because the vibration is affected by the narrowed feed channel due to foulant accumulation (as shown in Fig. 1) more than the changes in flux and salt rejection due to fluctuated salt concentration in the feed.

This is a very important discovery because the vibration sensor can figure out the starting point of fouling even in the condition where other parameters affecting water and salt permeability of the membrane are varied. Since a vibration sensor is usually attached to the high-pressure pump to monitor the possible failures such as cavitation as discussed earlier, the prediction of fouling is possible without installing any additional apparatus. What we need to do is just analyzing the vibration data from the existing sensors.

4. Conclusions

This work was motivated by (1) the difficulty in detecting early fouling in the condition where operation parameters like temperature and salt rejection of feed fluctuate and (2) the hypothesis that vibration signal may be changed due to the accumulated foulants inside the feed channel of the membrane module. The hypothesis was successfully verified by the lab-scale test followed by the vibration data analysis. The early fouling in terms of the vibration data analysis can be defined as the period when the average of the vibration data drops by over some percentage compared to that in the no-fouling period. The vibration data analysis can figure out the early fouling not only in the constant-control test but also

in the variation test were detecting the occurrence of fouling is difficult due to the fluctuation of operation parameters such as feed salt concentrations.

Acknowledgment

This work was supported by the National Research Foundation of Korea (NRF) grant funded by the Korea government (MSIP; Ministry of Science, ICT & Future Planning) (No. 2017R1A2B4002990).

References

- [1] S. Kim, E.M.V. Hoek, Interactions controlling biopolymer fouling of reverse osmosis membranes, *Desalination*, 202 (2007) 333–342.
- [2] S. Lee, S. Kim, J. Cho, E.M.V. Hoek, Natural organic matter fouling due to foulant-membrane physicochemical interactions, *Desalination*, 202 (2007) 377–384.
- [3] S. Kim, S. Lee, E. Lee, S. Sarper, C.H. Kim, J. Cho, Enhanced or reduced concentration polarization by membrane fouling in seawater reverse osmosis (SWRO) processes, *Desalination*, 247 (2009) 162–168.
- [4] S. Kim, S. Lee, C.H. Kim, J. Cho, A new membrane performance index using flow-field flow fractionation (fl-FFF), *Desalination*, 247 (2009) 169–179.
- [5] K.B. Park, C. Choi, H.W. Yu, S.R. Chae, I. Kim, Optimization of chemical cleaning for reverse osmosis membranes with organic fouling using statistical design tools, *Environ. Eng. Res.*, 23 (2018) 474–484.
- [6] M. Kim, B. Park, Y.J. Lee, J.L. Lim, S. Lee, S. Kim, Corrected normalized permeate flux for a statistics-based fouling detection method in seawater reverse osmosis process, *Desal. Wat. Treat.*, 57 (2016) 24574–24582.
- [7] X. Jin, A. Jawor, S. Kim, E.M.V. Hoek, Effects of feed water temperature on separation performance and organic fouling of brackish water RO membranes, *Desalination*, 239 (2009) 346–359.
- [8] ASTM, Standard Practice for Standardizing Reverse Osmosis Performance Data, D 4516-00 ASTM.
- [9] M.A. Saad, Early discovery of RO membrane fouling and real-time monitoring of plant performance for optimizing cost of water, *Desalination*, 165 (2004) 183–191.
- [10] M. Safar, M. Jafar, M. Abdel-Jawad, S. Bou-Hamad, Standardization of RO membrane performance, *Desalination*, 118 (1998) 13–21.
- [11] L.N. Sim, T.H. Chong, A.H. Taheri, S.T.V. Sim, L. Lai, W.B. Krantz, A.G. Fane, A review of fouling indices and monitoring techniques for reverse osmosis, *Desalination*, 434 (2018) 169–188.
- [12] J.S. Ho, L.N. Sim, R.D. Webster, B. Viswanath, H.G.L. Coster, A.G. Fane, Monitoring fouling behaviour of reverse osmosis membranes using electrical impedance spectroscopy: a field trial study, *Desalination*, 407 (2017) 74–84.
- [13] J.S. Vrouwenvelder, J.A.M. van Paassen, L.P. Wessels, A.F. van Dam, S.M. Bakker, The membrane fouling simulator: a practical tool for fouling prediction and control, *J. Membr. Sci.*, 281 (2006) 316–324.
- [14] J.S. Vrouwenvelder, M.C.M. van Loosdrecht, J.C. Kruithof, Early warning of biofouling in spiral wound nanofiltration and reverse osmosis membranes, *Desalination*, 265 (2011) 206–212.
- [15] G. Mousmoulis, N. Karlsen-Davies, G. Aggidis, I. Anagnostopoulos, D. Papantonis, Experimental analysis of cavitation in a centrifugal pump using acoustic emission, vibration measurements and flow visualization, *Eur. J. Mech. B. Fluids*, 75 (2019) 300–311.
- [16] A.R. Al-Obaidi, Investigation of effect of pump rotational speed on performance and detection of cavitation within a centrifugal pump using vibration analysis, *Heliyon*, 5 (2019) e019103.

- [17] A.K. Panda, J.S. Rapur, R. Tiwari, Prediction of flow blockages and impending cavitation in centrifugal pumps using support vector machine (SVM) algorithms based on vibration measurements, *Measurement*, 130 (2018) 44–56.
- [18] X. Su, W. Li, A. Palazzolo, S. Ahmed, Permeate flux increase by colloidal fouling control in a vibration enhanced reverse osmosis membrane desalination system, *Desalination*, 453 (2019) 22–36.
- [19] M. Kim, M. Kim, B. Park, S. Kim, Changes in characteristics of polyamide reverse osmosis membrane due to chlorine attack, *Desal. Wat. Treat*, 54 (2015) 923–928.
- [20] Sequoia IT S.R.L., Available at: <http://www.sequoia.it/wp/en>.
- [21] The R Project for Statistical Computing, Available at: <http://www.r-project.org>.